REPORT DOCUMENTATION PAGE

Form Approved
OMB No. 0704-0188

1. REPORT DATE *(DD-MM-YYYY)*	**2. REPORT TYPE**	**3. DATES COVERED** *(From - To)*
October 2012	Journal Article	October 2012- December 2012

4. TITLE AND SUBTITLE
Time-Synchronized Continuous Wave Laser-Induced Fluorescence Velocity Measurements of a Diverging Cusped Field Thruster

5a. CONTRACT NUMBER
In-House

5b. GRANT NUMBER

5c. PROGRAM ELEMENT NUMBER

6. AUTHOR(S)

Natalia A. MacDonald, Mark A. Cappelli and William A. Hargus, Jr.

5d. PROJECT NUMBER

5e. TASK NUMBER

5f. WORK UNIT NUMBER
Q0AZ

7. PERFORMING ORGANIZATION NAME(S) AND ADDRESS(ES)

Air Force Research Laboratory (AFMC)
AFRL/RQRS
1 Ara Drive.
Edwards AFB CA 93524-7013

8. PERFORMING ORGANIZATION REPORT NO.

9. SPONSORING / MONITORING AGENCY NAME(S) AND ADDRESS(ES)
Air Force Research Laboratory (AFMC)
AFRL/RQR
5 Pollux Drive
Edwards AFB CA 93524-7048

10. SPONSOR/MONITOR'S ACRONYM(S)

11. SPONSOR/MONITOR'S REPORT NUMBER(S)
AFRL-RQ-ED-JA-2012-457

12. DISTRIBUTION / AVAILABILITY STATEMENT
Distribution A: Approved for Public Release; Distribution Unlimited. PA#13014

13. SUPPLEMENTARY NOTES
Journal Article for the Journal of Physics D

14. ABSTRACT

Measurements are presented of time-synchronized ion velocities at three points within the acceleration channel and in the plume of a diverging cusped field thruster operating on xenon. Xenon ion velocities for the thruster are derived from laser-induced fluorescence measurements of the $5d[4]_{7/2}-6p[3]_{5/2}$ xenon ion excited state transition centered at λ = 834.72 nm. The thruster is operated in a high current mode, where the anode discharge current is shown to oscillate quasi-periodically. A sample-hold scheme is implemented to correlate ion velocities to phases along the current cycle. These time-synchronized measurements show that ionization and acceleration regions of the discharge shift in position over the course of a current cycle.

15. SUBJECT TERMS

16. SECURITY CLASSIFICATION OF:			**17. LIMITATION OF ABSTRACT**	**18. NUMBER OF PAGES**	**19a. NAME OF RESPONSIBLE PERSON**
					William Hargus
a. REPORT	**b. ABSTRACT**	**c. THIS PAGE**	SAR	15	**19b. TELEPHONE NO** *(include area code)*
Unclassified	**Unclassified**	**Unclassified**			661-525-6795

Standard Form 298 (Rev. 8-98)
Prescribed by ANSI Std. 239.18

Time-Synchronized Continuous Wave Laser-Induced Fluorescence Velocity Measurements of a Diverging Cusped Field Thruster

N A MacDonald,[1,2] M A Cappelli,[1] and W A Hargus, Jr.[2]

[1] Stanford Plasma Physics Laboratory, Stanford University, Stanford, CA 94305.
[2] In-Space Propulsion Branch, Air Force Research Laboratory, Edwards AFB, CA 93524.

‡

E-mail: natalia.macdonald@edwards.af.mil

Abstract. Measurements are presented of time-synchronized ion velocities at three points within the acceleration channel and in the plume of a diverging cusped field thruster operating on xenon. Xenon ion velocities for the thruster are derived from laser-induced fluorescence measurements of the $\mathbf{5}\boldsymbol{d}[\mathbf{4}]_{\mathbf{7/2}} - \mathbf{6}\boldsymbol{p}[\mathbf{3}]_{\mathbf{5/2}}$ xenon ion excited state transition centered at $\boldsymbol{\lambda} = 834.72$ nm. The thruster is operated in a high current mode, where the anode discharge current is shown to oscillate quasi-periodically. A sample-hold scheme is implemented to correlate ion velocities to phases along the current cycle. These time-synchronized measurements show that ionization and acceleration regions of the discharge shift in position over the course of a current cycle.

1. Introduction

This paper provides results of time-synchronized laser-induced fluorescence (LIF) velocimetry of an oscillatory cusped field plasma discharge operating on xenon. A continuous wave (CW) diode laser is used to probe the $5d[4]_{7/2} - 6p[3]_{5/2}$ xenon ion excited state transition centered at $\lambda = 834.72$ nm. A sample-hold circuit and lock-in amplifier are used to pull out fluorescence excitation lineshapes that each correspond to a particular point in time along the discharge current cycle.

This work is motivated by previous time-averaged LIF velocimetry measurements on the Diverging Cusped Field Thruster (DCFT).[1] The DCFT tends to operate in two modes:[2] a high current mode, characterized by quasi-periodic discharge current oscillations; and a low current mode that is quiescent. Differences in the time-averaged velocity maps between the two modes include the presence of a widely distributed acceleration region and diffuse plume during the high current mode that are not seen in the low current mode. These characteristics may be indicative of a fluctuation in the position of the ionization and acceleration regions in the plume due to the strong, low

frequency (~ 3 kHz) discharge current oscillations of the high current mode. While time-averaged measurements provide a good representation of the ion velocities throughout a quiescent discharge, a time-dependent velocity diagnostic is necessary for resolving the ion dynamics seen in the high current mode of operation.

Time-resolved LIF measurements typically employ pulsed dye lasers to study properties such as the spectral line broadening of a given transition, reflecting the temperature, velocitiy distribution, etc. However, the discharge in this work is operated on xenon, which has spectral linewidths that are too narrow to be resolved with a pulsed dye laser. The $5d[4]_{7/2} - 6p[3]_{5/2}$ xenon ion transition used in this work has a measured linewidth (a convolution of the natural linewidth of the transition and the velocity distribution function (VDF) for a given time in the discharge current cycle) on the order of 1.5 to 2.5 GHz. State of the art pulsed dye lasers that have linewidths >1 GHz[3] at best. In comparison, CW lasers with linewidths <300 kHz[3] are sufficiently narrow to resolve the transition's spectral features, and are therefore more desirable for making time-synchronized fluorescence measurements.

In recent years, several studies have attempted time-resolved CW-LIF measurements in oscillatory plasma discharges such as Hall thrusters. These include measurements of the time evolutions of ion velocity profiles for a Hall thruster after short interruptions to the thruster discharge power,[4, 5] or whose oscillations are driven at a particular frequency by a variable cathode current injection.[6] Our method[8, 7] varies from these studies in several important ways. First, it is intended for use on a quasi-periodic oscillatory mode of the DCFT discharge, operated continuously and without any alteration to the naturally occurring frequency. The oscillations in the DCFT are a result of the accumulation of ions within the thruster channel and subsequent expulsion of the ions due to an applied electric field. Without being driven at a constant frequency, these oscillations are quasi-periodic, with a frequency that tends to drift slightly over the course of a laser scan. Second, by using phase sensitive detection that is locked to a fixed mechanical chopper frequency, and a sample-hold circuit that triggers time-synchronization when the discharge current passes through a particular level, not at a particular frequency, we are able to extract fluorescence signals correlated to discharge currents that are not perfectly periodic. In contrast, the photon-counting technique used in the aforementioned studies[9] is more reliant on the periodicity of the discharge oscillations due to the straight addition and subtraction of fluorescence and background photons, respectively.

2. Experiment

2.1. Diverging Cusped Field Thruster

The DCFT is a plasma accelerator that was developed in an effort to address issues such as erosion that are seen when scaling traditional annular Hall thrusters to low power. A schematic of the DCFT is shown in Fig. 1a.[10] The acceleration channel in the DCFT

has a diverging, cone shape that is lined with permanent samarium cobalt (SmCo) magnets of alternating polarity. These magnets create a cusped magnetic field profile that is largely in the axial direction, with radial components at the magnet interfaces.

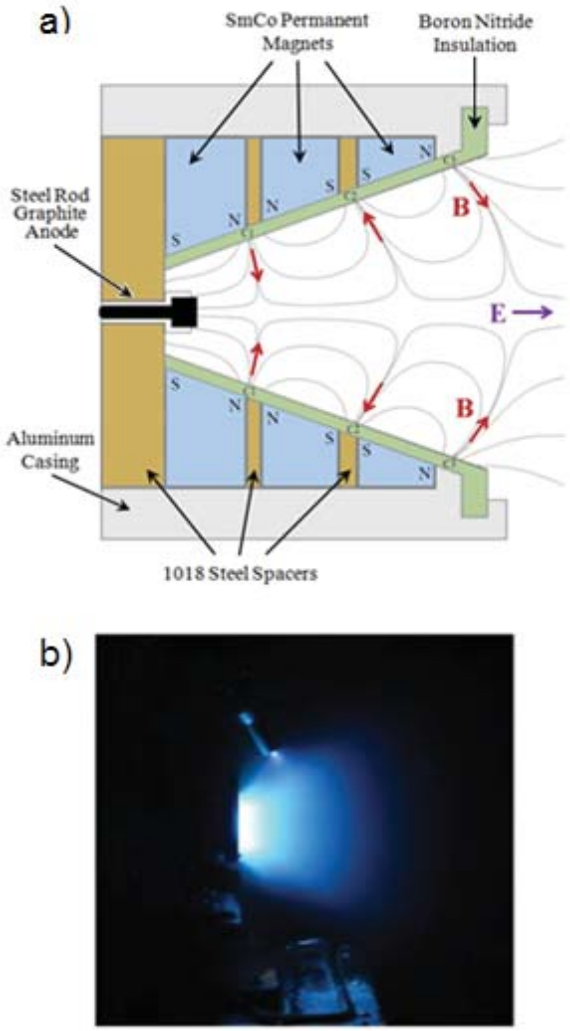

Figure 1. Diverging Cusped Field Thruster, developed by MIT. a) Schematic of DCFT, b) Operation in high current mode.

At the magnetic interfaces, the radially pointing magnetic field and axial electric field create a closed $\vec{E} \times \vec{B}$ electron drift, allowing for significant propellant ionization from electron bombardment. The closed electron drift also prevents electrons from directly reaching the anode, establishing a strong axial electric field that accelerates ions out of the thruster. In addition to these Hall thruster-like ionization and acceleration mechanisms, the cusped magnetic fields in these devices produce strong magnetic gradients that act on the charged particles in the thruster channel. These gradients result in a magnetic bottle effect for incoming electrons, trapping them between cusps where they mirror back and forth. Due to this magnetic mirror effect, the majority of charged particles (both ions and electrons) are prevented from reaching the thruster

walls. This minimizes wall erosion, a limiting factor in thruster lifetime. The magnetic bottles also further mitigate electron mobility directly to the anode, and add to the propellant ionization efficiency from the electron $\vec{E} \times \vec{B}$ drift. Further details of the design, including the magnetic field topology, can be found elsewhere.[10]

As described above, the DCFT tends to operate in either a high current or low current mode. The high current mode is characterized by periodic oscillations in the discharge current, while the low current mode is quiescent. This work focuses only on the high current mode, shown Fig. 1b, with the operating condition described in Table 1.

Table 1. DCFT operating condition during time-synchronized measurements.

Anode Flow	830 $\mu g/s$ Xe (8.5 sccm)
Cathode Flow	150 $\mu g/s$ Ar (4.75 sccm)
Anode Potential	300 V
Anode Current	0.49 A
Keeper Current	0.50 A
Heater Current	7.0 A

Based on the current trace in Fig. 2 and optical observations,[2] the oscillatory nature of the high current mode has been attributed to three distinguishable phases within each current cycle:

(i) Fast ionization of neutrals throughout the region accessible to the plasma.

(ii) Evacuation of ions from the downstream end of the formed plasma, with simultaneous electron evacuation to the anode.

(iii) Gradual re-fill of neutrals in the thruster channel.

As shown in Fig. 2, increases in discharge current are mirrored by slight decreases in anode potential, resulting in an anode power spikes that go as high as 570 W while the average is 147 W.

These oscillations in some ways emulate the breathing mode seen in traditional Hall thrusters [11, 12]. In Hall discharges, current oscillations are directly associated with the periodic depletion of the neutral atom density in the ionization zone near the thruster exit.[13] However, typical breathing mode frequencies for Hall thrusters are in the 15-20 kHz range, whereas the oscillations seen in the DCFT are on the order of 3 kHz. This difference in frequency raises the question: are the discharge oscillations in fact analogous to the breathing mode of a Hall thruster? More specifically, are the ionization and peak acceleration regions fluctuating in position in the thruster channel as the discharge current oscillates? Or is the acceleration region just distributed over a wider portion of the thruster channel, as seen in the time-averaged velocity measurements?[1] A time-resolved or time-synchronized CW-LIF method will help make this distinction.

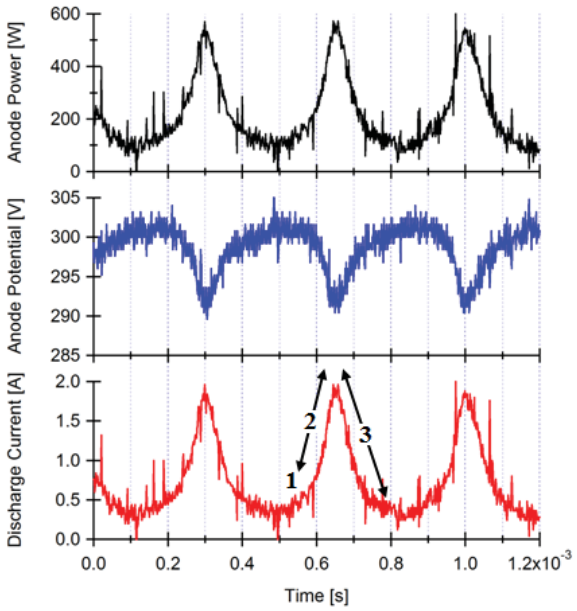

Figure 2. Anode current, voltage and power traces for the oscillatory operating mode of the DCFT. Numbers 1 to 3 in the lower trace describe the three phases within the current cycle.

2.2. Experimental Apparatus

Thruster LIF measurements are performed in the large vacuum chamber facility at the Stanford Plasma Physics Laboratory (SPPL). The base pressure in the chamber is 4×10^{-7} Torr and 1×10^{-5} Torr with a thruster running at nominal conditions.

Ion velocity measurements are accomplished by probing the $5d[4]_{7/2} - 6p[3]_{5/2}$ electronic transition of Xe II at 834.72 nm. The upper state of this transition is shared by the $6s[2]_{3/2} - 6p[3]_{5/2}$ transition at 541.92 nm[14], which is used in this study for non-resonant fluorescence collection. This transition has been used extensively throughout the electric propulsion community for time-averaged LIF velocimetry measurements,[15, 16, 17, 18] including previous work on the DCFT.[1] Ion velocities are determined by measuring the Doppler shift of the absorbing ions[19].

Figure 3 depicts the LIF optical system. The lower left-hand portion shows the probe optics before they enter the vacuum chamber. The laser is a New Focus Vortex $TLB-6017$ tunable CW diode laser, with a center wavelength of 834.7 nm. The laser is typically scanned over an ∼20 GHz frequency range to encompass an entire spectral feature as well as a nearby reference line. The 10 mW beam is passed through several beam pick-offs for diagnostic purposes. The first beam pick-off directs a beam to a photodiode detector (D1) used to provide constant power feedback to the laser. The second beam is divided into two equal components by a 50-50 cube beam splitter. The first component is directed to a Burleigh WA-1500 wavelength meter used to monitor absolute wavelength. The second component is sent through a low pressure xenon hollow cathode discharge lamp (HCL), that provides a wavelength reference through absorption

of the neutral xenon $6s'[1/2]_1^0 - 6p'[3/2]_2$ transition at 834.68 nm [20, 21]. The second pick-off sends a beam to a Thorlabs SA200 Fabry-Perot etalon (F-P), with a 1.5 GHz free spectral range and finesse of 200. Combined with the absorption reference, the F-P etalon provides a high resolution frequency measurement that gives a much more accurate measurement of wavelength than the wavemeter as the laser is swept during a scan.

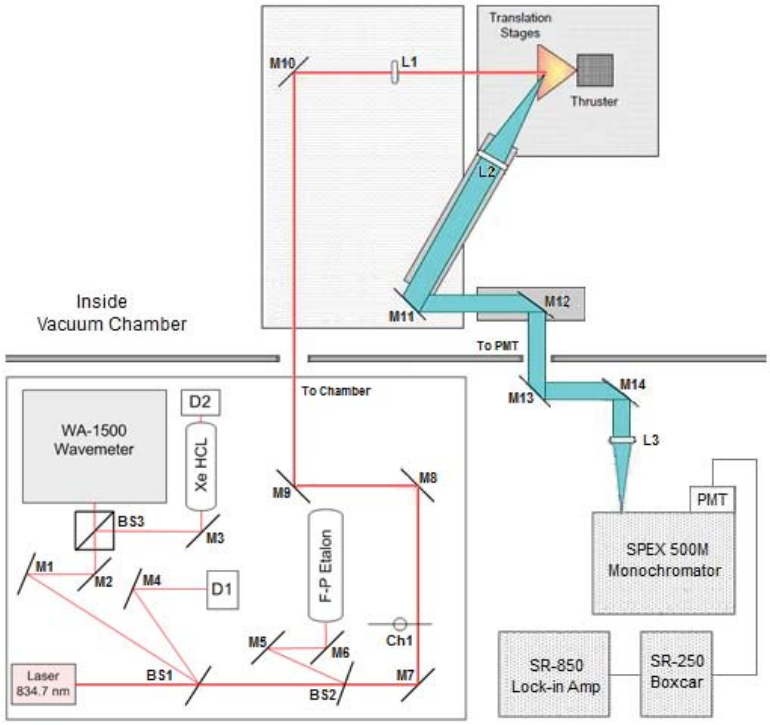

Figure 3. Top view diagram of the laser optical train and collection optics for time-synchronized thruster LIF measurements at SPPL. BS = Beam Splitter; Ch = Chopper; D = Diode; L = Lens; M = Mirror.

The main portion of the beam is sent through a Stanford Research Systems SR540 mechanical chopper, rotating at 400 Hz for phase sensitive detection. Once inside the vacuum chamber, the beam is directed such that it probes axial ion velocities in the thruster. The fluorescence signal is collected by a 75 mm diameter plano-convex lens with a focal length of 250 mm. This lens is oriented 45° from the axial probe beam axis, a distance of 250 mm from the intersection with the probe beams, to minimize interactions with the plume (i.e. sputtering on the optics). The collected light is directed out of the vacuum chamber by a series of mirrors, and is then focused into a 750 mm focal length monochromator with a photomultiplier tube (PMT) by a second 75 mm diameter plano-convex lens with a focal length of 250 mm. The collection optics have a 1:1 magnification, which allows the spatial resolution of the measurements to be determined by the diameter of the probe beam (1 mm) and the image of the entrance slit (0.8 mm width by 0.2 mm height) that defines the collection optics solid angle. If sent directly into a lock-in amplifier, the resulting signal would be a time-averaged

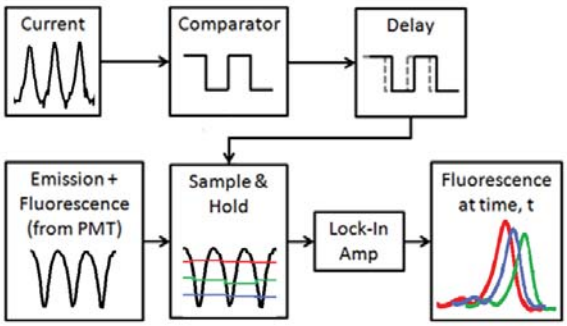

Figure 4. Block diagram of the sample-hold method of synchronizing the fluorescence trace to various times along a discharge current cycle.

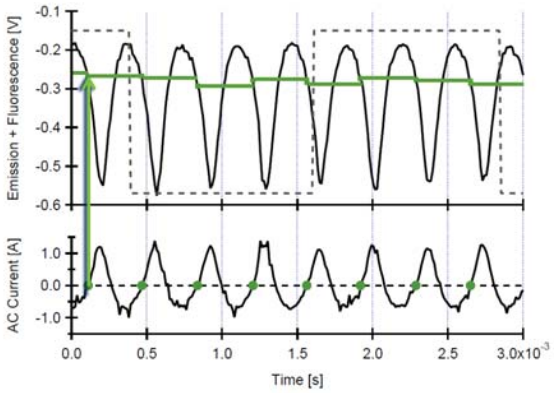

Figure 5. Raw PMT and AC current traces for the DCFT discharge. Arrow indicates the correlation between points in current cycle (bottom) and sample-held signal from the emission plus fluorescence trace (top) for time = t_0. Chopper frequency (- - -) is shown for reference. Note: the emission plus fluorescence signal is negative due to the negatively applied bias on the PMT.

measurement of the fluorescence excitation lineshape.

To synchronize the LIF signal in time to the discharge current, a sample-hold scheme is implemented between the PMT and the lock-in amplifier. The development of this sample-hold scheme is described elsewhere.[7] Fig. 4 provides a block diagram of the sample-hold method. Simultaneous measurements are made of the AC discharge current, absorption reference, etalon, and emission plus fluorescence signal from the PMT, as the CW laser is scanned slowly in wavelength across the spectral feature. Due to the large background emission and associated noise, laser scans typically take on the order of 30 minutes to achieve adequate signal-to-noise for the fluorescence excitation lineshape.

The AC measurement of discharge current is fed into an LM339 comparator chip. Points where the current passes through zero with a positive slope trigger the comparator, resulting in a series of transistor-transistor logic (TTL) pulses with an approximately 50% duty cycle. The comparator signal and raw emission plus fluorescence signal from the PMT are then fed into an SRS SR-250 Boxcar Averager

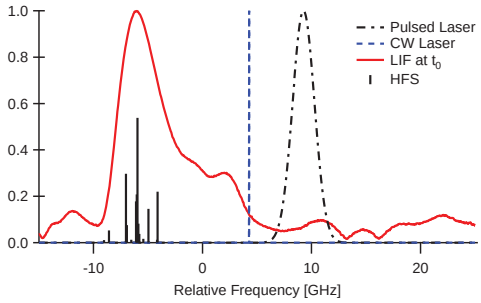

Figure 6. Fluorescence excitation lineshape at time t_0 at a position $X = -8$ mm, $Z = 0$ mm in the plume of the DCFT, as compared to the width of a typical CW laser and a pulsed dye laser. The hyperfine structure (HFS) of the transition is shown for reference.

where the sample-hold function is performed.

For every positive slope in the comparator signal, the boxcar averager samples the PMT signal for a period of time defined by the gate width. The last sampled value of the PMT signal is held until the next comparator trigger, at which point the boxcar averager re-samples and holds the PMT signal. Fig. 5 provides an example of how the zero point crossings of the AC discharge current correlate to points in the sample-held emission plus fluorescence signal. This process is repeated throughout the length of the laser scan, resulting in the "sample-held" signal.

The sample-held signal is then fed into an SRS SR-850 Lock-in Amplifier with the chopper reference frequency for phase sensitive detection, resulting in a fluorescence excitation lineshape synchronized to time t_0 in the current discharge cycle. To sample additional times along the current cycle, the built in time delay in the SR-250 is used to adjust the sample trigger before the laser scan is repeated.

Figure 6 provides a fluorescence excitation lineshape for time t_0 at a position of $X = -8$ mm, $Z = 0$ mm in the plume of the DCFT. The linewidths for a CW and a pulsed dye laser, as well as the hyperfine structure (HFS) of the probed transition are also shown for reference. As mentioned previously, these line widths illustrate the need for a CW laser when resolving this spectral feature.

3. Results and Discussion

Figure 7 provides the three measurement locations used in the time-synchronized study of the DCFT. Point 1 at R = +8 mm, Z = -16 mm, is inside the thruster channel near the separatrix defined by the second cusp, marked as C2. This point is in the brightest region of the plume, and is likely near a region of high ionization inside the thruster channel. Point 2, at R = +8 mm, Z = 0 mm, is at the exit plane of the thruster near the outermost separatrix defined by the third cusp, C3. Point 2 is near the region of highest measured potential drop, where the majority of ion acceleration begins. Point 3, at R = +16 mm, Z = +4 mm, is at the beginning of the jet region of the plume after

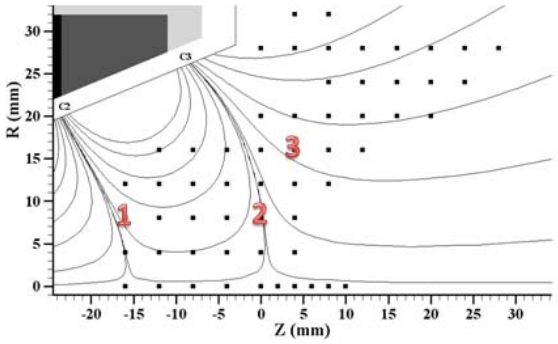

Figure 7. Positions of the three time-synchronized LIF measurements on the DCFT.

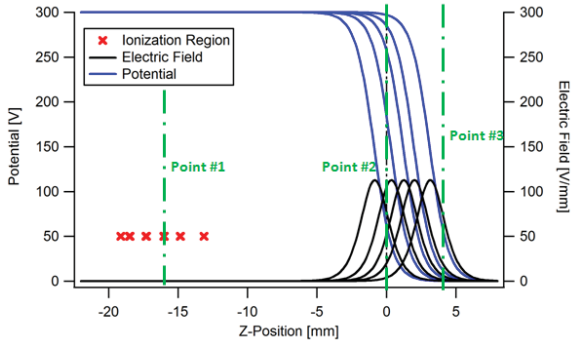

Figure 8. 1-D simulation of ionization and acceleration regions used to describe the velocities at three points in the DCFT plume. Note: magnetic field effects are neglected.

the majority of the potential drop.

These points were chosen based on the time-averaged DCFT velocity measurements presented in previous work[1]. In these measurements, the DCFT's high current mode revealed axial acceleration beginning as deep as Z = -12 to -16 mm in the thruster channel (near the second cusp). This is in contrast to the quiescent, low current mode of operation, in which the majority of ion acceleration was localized just inside the thruster exit plane (near the third cusp). The deeper distribution of the high current mode's ionization region may indicate a fluctuation in the position of the ionization front in conjunction with the current oscillations. Movement of the ionization region could also cause the position of the peak electric field to fluctuate around its average position, which is at approximately Z = +2 mm into the plume.

From these observations and predictions, a 1-D simulation of the measurement locations (Z-coordinate only) was made to predict how the ionization at acceleration regions may shift over the course of a current cycle. This simulation is depicted in Fig. 8. Results of this simulation are compared to the time-synchronized velocity measurements that follow.

Figures 9 through 11 provide typical time-syncronized lineshapes for the measurement locations at several points in time along the discharge current cycle.

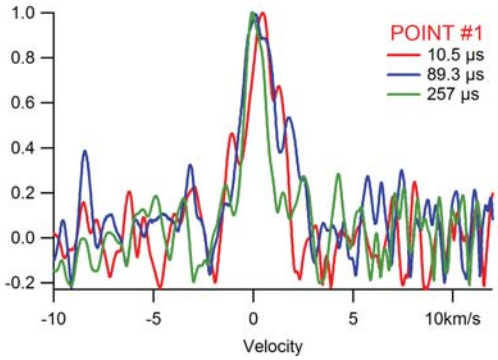

Figure 9. Fluorescence excitation lineshapes at various times along a discharge current cycle for R = +8 mm, Z = -16 mm in the DCFT channel.

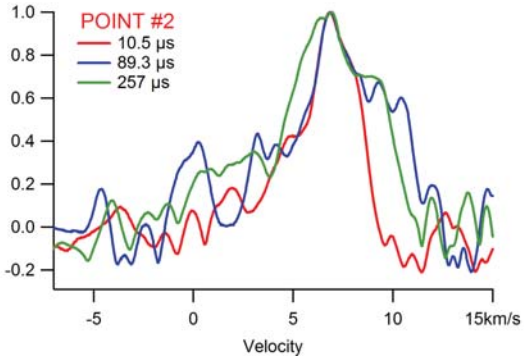

Figure 10. Fluorescence excitation lineshapes at various times along a discharge current cycle for R = +8 mm, Z = 0 mm, at the exit of the DCFT channel.

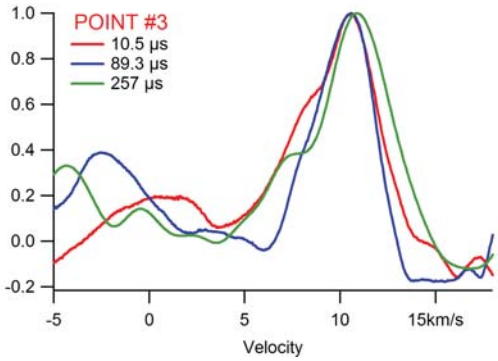

Figure 11. Fluorescence excitation lineshapes at various times along a discharge current cycle for R = +16 mm, Z = +4 mm in the plume of DCFT discharge.

While the positions of the measured lines have proven repeatable, the low signal to background ratio (estimated at 1/15,700 before going into the lock-in amplifier) merits further work with increased laser power, faster optics, longer scan lengths, etc. before velocity distribution functions can be extracted.

Gaussian fits to the time-synchronized lineshapes provide the most probable axial ion velocities for each given position and time. The most probable velocities are

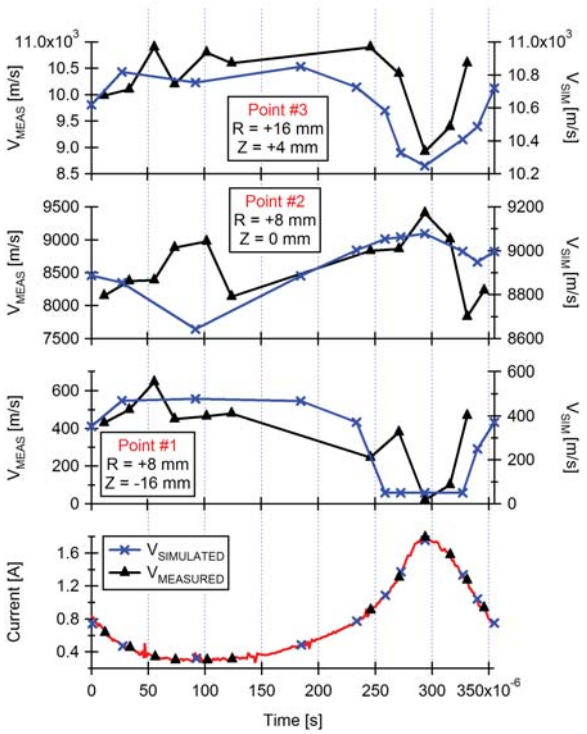

Figure 12. Measured most-probable axial ion velocities as a function of the discharge current for three points in the plume of the DCFT. Axial ion velocities from 1-D simulation are shown for comparison.

summarized in Fig. 12, and are compared to results from the 1-D simulation described above.

At Point 1, around which the ionization region is assumed to fluctuate, higher axial velocities are seen at times when ions are born deeper in the discharge channel. As the discharge current reaches its peak and the ionization region moves closer to the exit plane, the ions observed at Point 1 have traveled through less of a potential drop, and have therefore achieved a lower axial velocity.

At Point 2, the peak potential drop is assumed to fluctuate back and forth over the measurement location. This point reveals a bi-modal change in velocity, where the velocities reach their peaks at the maximum and minimum of the current cycle, corresponding to the times when the peak potential drop is farthest upstream and downstream of the measurement location, respectively. The peak in velocity when the potential drop begins upstream of Z = 0 matches the trend seen in Points 1 and 3, as the ions have seen most of the potential drop by the time they reach the exit plane. The second velocity peak, when the ions have not yet seen the full potential drop, is opposite of that seen in Points 1 and 3, and appears to be coupled to where the ions are born. For example, ions born further downstream towards the exit plane may see a larger potential drop immediately, while those born upstream in a region of weaker electric field may travel some distance down the thruster channel at speeds closer to the thermal velocity of the neutrals before being accelerated by the strong electric field.

By Point 3, the majority of ions have seen the full potential drop and are continuing outwards from the separatrix on ballistic trajectories determined in regions similar to Point 1 and 2. Only at points when the discharge current is maximum, and the peak electric field is shifted outwards from Z = +2 mm, does the velocity dip below that achieved by the full potential drop.

As shown in Fig. 12, the measurements and simulation show similar results, with comparable average velocities and patterns for how the velocities change over the course of the discharge current cycle. Notable differences include the span between minimum and maximum velocities at a given point is on the order of 300-800 m/s in the simulation, whereas it can be as large as 2,500 m/s for the measurements. And for Point 2, while the simulation shows a peak in velocity at the beginning of the current cycle, it does not quite match the time when this peak occurs in the measurements. These differences are artifacts of needing a more comprehensive model (that is 2-dimensional and may include magnetic field effects) in order to better match the velocities seen in this discharge.

Overall, the velocities of the ions at each measurement location appear directly related to a shifting in position of ionization and acceleration regions that is correlated with the discharge current fluctuations. Although the discharge oscillations in the DCFT are of much lower frequency than a typical Hall thruster breathing mode ($\sim$3 kHz, as compared to 15-20 kHz), they appear to be caused by a similar mechanism in the discharge.

In a Hall thruster breathing mode, the high magnetic field in the ionization zone traps electrons, resulting in low mobility across the magnetic field lines. In order to maintain current continuity across the thruster, the electric field increases in this region, giving more energy to electrons such that they can escape the magnetic field lines and ionize neutral atoms. The number of neutrals decreases near the channel exit due to the high ionization rate caused by the bombardment by high energy electrons. This moves the front of the region with high neutral density upstream in the channel to a region of lower magnetic and electric field, and therefore lower electron energy and ionization rate. With fewer neutrals left to ionize, the plasma density near the channel exit starts to decrease. The decrease in plasma density causes a decreased electron flux at the channel exit. This allows the neutrals to re-fill the ionization zone without all becoming ionized. The process repeats itself in what is often termed a "predator-prey" fluctuation.[13]

Unlike in a Hall thruster, the magnetic fields lines in the DCFT are not entirely radial in direction and their strength increases upstream towards the anode with the strongest magnetic fields located at the cusps. Therefore, when the ionization region recedes towards the second cusp and anode (like in a Hall thruster), it may be forced back towards the third, outermost cusp where the magnetic field strength is lower. causing the ionization front to jump back and forth between the second and third cusps. This may indicate that there are additional factors contributing to the oscillations.

Previous work has shown that there are several contributing factors to the breathing mode oscillation frequency.[11] These include the propellant mass flow rate and applied

anode potential, which influence the neutral re-fill rate and ion acceleration, respectively, and the magnetic field strength, where increasing magnetic field decreases electron mobility and thereby the oscillation frequency. In terms of the DCFT, measurements in the high current mode have shown that changing the xenon mass flow rate from 9 to 7.5 sccm (880 to 740 μg/sec), with a fixed 300 V anode potential, causes the frequency to decrease from 3.6 kHz to 2.7 kHz. The magnetic field strengths seen in the DCFT are on the order of 0.5 Tesla, which is 5 to 10 times stronger than seen in typical Hall thrusters. The lower frequency discharge oscillations of the DCFT would therefore be expected. These observations in conjunction with the time-synchronized LIF velocity measurements indicate that the DCFT high-current mode is similar to a Hall thruster breathing mode.

4. Conclusions

A sample-hold with phase sensitive detection method of time-synchronized CW laser-induced fluorescence was presented. Time-synchronized ion velocity measurements were presented at several positions in the plume of the DCFT, operating in its oscillatory high-current mode. These measurements revealed that ion velocities in the DCFT are directly correlated to the phase of the discharge current oscillations, whereas the time-averaged velocity measurements were unable to resolve these dynamics.

The current and velocity fluctuations seen in the high current mode of the DCFT appear to be similar to the ionization instability seen in traditional Hall thrusters, known as a "breathing mode." The position of the ionization region likely fluctuates back and forth between the second and third magnetic cusps in the discharge channel. The location of the maximum potential drop also appears to fluctuate, proportional to the current oscillations and centered around Z = +2 mm into the plume where time-averaged LIF measurements place the peak electric field.

Acknowledgments

N. MacDonald acknowledges the Science Mathematics and Research for Transformation (SMART) scholarship program for support of her research. Research at Stanford is funded through the Air Force Office of Scientific Research with Dr. M. Birkan as grant monitor.

5. References

[1] N. A. MacDonald, M. A. Cappelli, S. R. Gildea, M. Martinez-Sanchez, and W. A. Hargus Jr. J. Phys. D **44**, 295203 (2011).

[2] S. R. Gildea and T. S. Matlock and P. Lozano and M. Martinez-Sanchez Low Frequency Oscillations in the Diverging Cusped-Field Thruster: Proceedings of the 46th AIAA/ASME/SAE/ASEE Joint Propulsion Conference & Exhibit, Nashville, TN, July 25-28, 2010, AIAA 2010-7014.

[3] Newport Corporation. Website. Accessed: 16 December 2011. http://www.newport.com.

[4] S. Mazouffre, D. Gawron, and N. Sadeghi. Phys. of Plasmas **16**, 1 (2009).
[5] S. Mazouffre, and G. Bourgeois. Plasma Sources Sci. Technol. **19**, 065018 (2010).
[6] K. Dannenmayer, P. Kudrna, M. Tichy, and S. Mazouffre. Plasma Sources Sci. Technol. **21**, 055020 (2012).
[7] N. A. MacDonald, M. A. Cappelli, and W. A. Hargus Jr. Rev. Sci. Instrum. **83**, 113506 (2012).
[8] Development of a Time Synchronized CW-Laser Induced Fluorescence Measurement for Quasi-Periodic Oscillatory Plasma Discharges: Bulletin of the 65th Annual Gaseous Electronics Conference, Austin, TX, October 22-26, 2012, Vol. 57, No. 8.
[9] B. Pelissier, and N. Sadeghi. Rev. Sci. Instrum. **67**, 3405 (1996).
[10] D. G. Courtney and P. Lozano and M. Martinez-Sanchez. Continued Investigation of Diverging Cusped Field Thruster: Proceedings of the 44th AIAA/ASME/SAE/ASEE Joint Propulsion Conference & Exhibit, Hartford, CT, July 21-23, 2008, AIAA 2008-4631.
[11] J. P. Boeuf and L. Garrigues. J. Appl. Phys. **84**, 3541 (1998).
[12] E. Y. Choueiri. Phys. Plasmas **8**, 1411-1426 (2001).
[13] J. Fife, M. Martinez-Sanchez and J. Szabo. A numerical study of low-frequency discharge oscillations in Hall thrusters: Proceedings of the 33rd AIAA/ASME/SAE/ASEE Joint Propulsion Conference & Exhibit, Seattle, WA, July 6-9, 1997, AIAA-1997-3052.
[14] J. E. Hansen, and W. Persson. Phys. Scr. **4**, 602 (1987).
[15] D. H. Manzella. Stationary Plasma Thruster Ion Velocity Distribution: Proceedings of the 30th AIAA/ASME/SAE/ASEE Joint Propulsion Conference & Exhibit, Indianapolis, IN, June 27-29, 1994, AIAA-1994-3141.
[16] Hargus, Jr., W. A. and M. A. Cappelli. Appl. Phys. B **8**, 961 (2001).
[17] N. A. MacDonald, C. V. Young, M. A. Cappelli, and W. A. Hargus, Jr. J. Appl. Phys. **111**, 093303 (2012).
[18] S. Mazouffre, D. Gawron, V. Kulaev, and N. Sadehgi. IEEE Trans. Plasma Sci. **36**, 1967 (2008).
[19] W. Demtroder, Laser Spectroscopy: Basic Concepts and Instrumentation (Springer-Verlag, Berlin, 1996).
[20] M. H. Miller, and R. A. Roig. Phys. Rev. A **8**, 480 (1973).
[21] C. E. Moore. Atomic Energy Levels. vol. II (National Bureau of Standards, Gaithersburg, MD, 1958).